[Short title + Author Name - P&H title] 32 (2024) 101932

HOSTED BY

ELSEVIER

Contents lists available at ScienceDirect

Saudi Pharmaceutical Journal

journal homepage: www.sciencedirect.com

Original article

Anti-quorum sensing activity of poly-amidoamine dendrimer generation 5 dendrimer loaded kinase inhibitor peptide against methicillin-resistant *Staphylococcus aureus*

Naifa A. Alenazi [a,*], Fadilah S. Aleanizy [a], Fulwah Y. Alqahtani [a], Abdullah A. Aldossari [b], Mohammed M. Alanazi [b], Rihaf Alfaraj [a]

[a] *Department of Pharmaceutics, College of Pharmacy, King Saud University, Riyadh 11495, Saudi Arabia*
[b] *Department of Pharmacology and Toxicology, College of Pharmacy, King Saud University, Riyadh 11495, Saudi Arabia*

ARTICLE INFO

Keywords:
Methicillin-resistant *Staphylococcus aureus*
poly-amidoamine dendrimers (PAMAM)
Anti-virulence agent
Accessory gene regulator
Histidine kinase inhibitor

ABSTRACT

Methicillin-resistant Staphylococcus aureus (MRSA) is a significant concern in both healthcare and community settings, as it causes numerous infections worldwide with high morbidity and mortality rates. One promising strategy is to target the quorum sensing (QS) system of MRSA using a dendrimer loaded with kinase inhibitor peptide. The present investigation has formulated a poly-amidoamine dendrimer (PAMAM) G5 dendrimer that is loaded with Quorum Quencher (QQ) peptide, which functions as a histidine kinase inhibitor. The particle average size of the formulated G5-QQ3 complex was determined to be 276 nm, and polydispersity index values of 0.33. The MIC_{50} for the formulated nanoparticles was 18 μM as demonstrated by a growth assay. Furthermore, the G5-QQ3 complex was able to inhibit the hemolysis activity of the MRSA with a concentration of 10 μM, and for *Staphylococcus aureus* was 3 μM. The G5-QQ3 complex possesses the ability to inhibit, penetrate, and eradicate biofilm in MRSA, *Staphylococcus aureus*, and different *agr* mutants with inhibition percentages ranging from 60 to 72%. Furthermore, live/dead viability assay confirmed the ability of the formulated nanoparticles to effectively kill all strains within the biofilm structure as evidenced by a confocal microscope, and the cytotoxicity of the G5-QQ3 complex was dose-dependent ($p < 0.05$). against RAW 264.7 cells. In general, the study confirmed that encapsulating QQ3 peptide within PAMAM G5 dendrimer results in a potent anti-virulence and anti-bacterial action and suggests a synergistic effect. The findings of this study have significant implications for the development of new treatments for MRSA infections, which are a major public health concern.

1. Introduction

MRSA refers to methicillin-resistant *Staphylococcus aureus*, is the predominant pathogen contributing to antimicrobial resistance (AMR) in both community and healthcare settings. *S.aureus* is an opportunistic pathogen that can cause serious infections and is difficult to treat. Despite the continued advent of new antibiotics, MRSA continues to be one of the most persistent drug-resistant pathogens with high mortality rates. The CDC considered a wide range of factors, including treatability, mortality, burden on the healthcare infrastructure and the community, prevalence, and increasing trends of resistance, in addition to the drugs that are currently in the pipeline, and declared MRSA as a serious threat (Kadri, 2020). These resistance strains are responsible for many serious infections, including device-related infections, osteomyelitis, endocarditis, urinary tract infections, and skin soft tissue infections. Also, according to the World Health Organization (WHO), MRSA is classified as one of the 12 priority pathogens that threaten human health. In Saudi Arabia, the prevalence rate of MRSA is 38% and it is considered the highest among Gulf countries. The rate of MRSA prevalence in the Western 42%, Central 32%, and Eastern region was 27% (Aljeldah, 2020). The consequences of MRSA infection continue to increase, and the reasons for this increase include the increases in transmission rates, intense colonization, and rapid bacterial activation of virulence factors that increase the infection's pathogenicity (Al Bshabshe et al., 2020). Overuse of antibiotics has been associated with resistance in hospitals and communities. Antibiotic resistance is a serious and growing global threat that may herald the end of the antibiotic era. Resistance makes some of these antibiotics entirely

* Corresponding author.
E-mail address: Naifa.alenazi@gmail.com (N.A. Alenazi).

https://doi.org/10.1016/j.jsps.2023.101932
Received 30 November 2023; Accepted 18 December 2023
Available online 19 December 2023

ineffective, and it occurs incidentally by gene mutation or acquisition of the resistance gene from other bacteria by plasmid transfer (Grundstad et al., 2019). Quorum sensing (QS), is a mechanism that allows cell-to-cell communication due to the population expansion of the bacteria. In MRSA quorum-sensing accessory gene regulator (agr) systems control the virulence factors production. Therefore, at high cell density agr is activated leading to secret an auto-inducing peptide (AIP). These AIP are detected by the transmembrane receptor leading to activating the virulence factors to enhance the ability of the bacteria to cause infection. During the invasion, agr is activated, and colonization with MRSA has been associated with the downregulation of the agr system and diminished expression of toxins, but increased biofilm formation. Also, it has been reported that activation of the agr system is necessary for the detachment of biofilm. So, an agr system is necessary for the establishment and detachment of biofilm, it regulates the switch between planktonic and biofilm lifestyles (Grundstad et al., 2019). For biofilm established AIP is required that may activate the agr system, and for detachment extracellular proteases activity is needed, and the target of these agr -controlled genes is not clear. The biofilm formed by agr mutants is thicker and smoother than wild type (WT) (Chen et al., 2022).

MRSA pathogenicity is highly dependent on virulence factors such as toxins (Hemolysins), immune-evasive surface factors (capsule and protein A), and biofilm formation (Aljeldah, 2020). MRSA has two QS system produced by agr locus; RNAII originate from the P2 promoter, and RNAIII originate from P3 promoter. The RNAIII segment of agr is generated from four genes agrBDCA, which encode all the main components of the QS system. The transmembrane protein agrB involve in; AIP secretion, and agrD processing. Whereas agrA encodes the cytosolic response regulator (RR), and agrC encodes membrane-bound histidine kinase (HK) and both form the two-component regulatory system (AgrAC TCS) (Fihn and Carlson, 2021). TCs are tools to regulate the interaction, adaption to conditions, and survival in the human host environment. TCSs are highly conserved domine and the main signal transduction pathways the bacteria use to regulate many processes including metabolism, virulence, protein interaction, and antibiotic resistance (Fihn and Carlson, 2021). The agrC receptor-histidine protein kinase binds to AIPs and upon binding leads to phosphorylates of agrA in the cytosol. Then it will bind to P2 and P3 leading to stimulating the transcription of regulatory RNA-II, RNA-III, and expression of virulence factors. Therefore, the two-component system is important for bacterial life and death and is required for resistance to common antibiotics. This makes these components a promising target for discovering novel antibacterial activity. The inhibition of autophosphorylation of HK will result in a broad-spectrum antibacterial activity. Also, the folding of the CA domine in the HK in bacterial cells is different from the folding in the mammalian cell, this gives a selectivity for the inhibitor with reduced side effects (Choudhary et al., 2018). Increasing antibiotic resistance and diminishing the development of new antibiotics by the pharmaceutical industry represent a global crisis that creates a need for alternative anti-infective strategies. These resistance strains can cause serious infections that are difficult to treat, with limited medication options available. One of the new strategies for facing these resistance pathogens is by targeting the virulence factor in the bacteria.

A novel macrocyclic peptide was discovered by the Random non-standard Peptide Integrated Discovery (RaPID) system. This peptide was a potent agr quorum quencher and reduced the virulence factors in *S.aureus* by competitive binding to the sensor histidine kinase agrC and inhibiting its function (Xie et al., 2020). In agreement with previous studies (Prieto et al., 2020). HK of the TCS is an attractive target for antibacterial and anti-quorum sensing agents. Targeting virulence such as QS is a new strategy that will reduce the evolution of bacteria to develop resistance. Because it disrupts the upstream regulatory functions of the bacterial physiology and leads to suppressing a series of virulence factors. While conventional antibiotics target only a specific bacterial protein that will impair the downstream functions. Combining conventional antibiotics with drug targeting this system will result in an effective antimicrobial agent and the potential to develop resistance will be minimal (Zhou et al., 2019).

With their unique structure, dendrimers are considered a promising drug delivery system with reduced cytotoxicity. It is highly ordered branched macromolecules with well-defined, homogeneous 3-dimensional structures. Poly-amido-amine (PAMAM) dendrimers have accessible interiors that can be used to encapsulate molecules. They have antimicrobial properties and high drug-loading capacity (Janaszewska et al., 2019). Anionic and amphiphilic dendrimers can escape from the immune cell and provide target delivery for the infected cell. PAMAM-dendrimers conjugated with a membrane-interacting peptide were found to be active against herpes simplex virus and inhibit the virus replication. Another study used dendrimer antimicrobial peptides named G3KL was tested against multidrug resistance *P.aeruginosa* clinical isolates. The results demonstrate that induction of spontaneous resistant mutants with the dendrimer was difficult due to the fast-killing effect of the dendrimer (Studzian et al., 2020).

Treating MRSA infection is a huge challenge; the study developed a new strategy for treating MRSA strains with a new anti-virulence agent using nanotechnology. The study targeted the QS-system in MRSA by using a new quorum quencher (QQ) peptide (QQ3 Fig. 1) that considers a potential HKI of the TCS. Therapeutic peptides have a limitations, namely, such as inadequate in vivo stability. The study used PAMAM generation 5 (G5) dendrimers (1,4-diaminobutane core, carbomethoxypyrrolidone-terminated) with antimicrobial properties to encapsulate the QQ3-peptide for efficient drug delivery, enhanced potency and stability. Dendrimers often face a significant drawback, which is their toxicity. This is primarily attributed to the existence of primary amine (NH2) groups and the positive charge on their surface, enabling them to readily interact with the negatively charged constituents of cell membranes. Consequently, this interaction can lead to cell lysis and cytotoxicity. To address this concern, the study employs PAMAM G5 dendrimers that are terminated with carbomethoxypyrrolidone, aiming to enhance the biocompatibility of the dendrimer. The study confirms that encapsulating QQ3 peptide within PAMAM G5 dendrimer results in a potent anti-virulence and anti-bacterial action and suggests a synergism effect.

2. Materials and methods

2.1. Materials

Zetasizer Nano ZS90 (Malvern Instruments Ltd, UK) used to measure the zeta potential, polydispersity index (PDI), and particle size of the formed nanoparticles. Transmission electron microscopy (TEM) (JEM1230EX; Tokyo, Japan), QQ3 was obtained from Pepmic Co., Ltd (China). Polyamidoamine dendrimer generation 5 (PAMAM dendrimers G5, 1 g vial) (molecular formula; C2032H3300N506O636) was purchased from Nanosynthons (Mt. Pleasant, MI, USA), was purchased from Nanosynthons (Mt. Pleasant, MI, USA), RAW 264.7 a macrophage cell proliferation kit I (MTT) was provided from American Type Culture Collection (ATCC). Bacterial strains wild type and mutants obtained from the library of MRSA transposon from the University of Washington Genome Centre (Washington University, Washington, Seattle, USA).

2.2. Bacterial strains and growth condition

All bacterial strains listed in Table 1 were grown at 37 °C for 18–24 hr in Tryptic Soy Broth (TSB) and Tryptic Soy Agar (TSA) supplemented with erythromycin15 μg/mL as a selective marker was used.

2.3. Formulation of G5-QQ3 complex

Loading the QQ3 into the PAMAM dendrimer was achieved using a molar ratio of 1:1 for each. 1 g of G5 PAMAM dendrimers was dissolved into 10 ml of Milli-Q water to give a concentration of (10% w/v) and

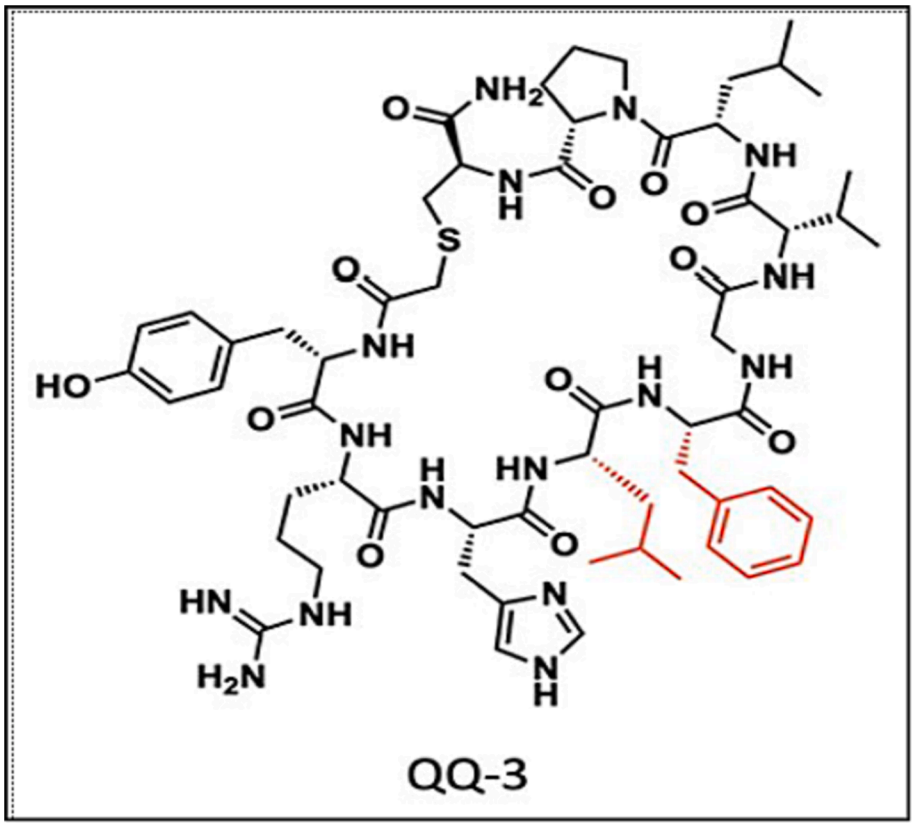

Fig. 1. One of the new quorum quencher (QQ) peptide QQ3 (Xie et al., 2020).

Table 1
Strains used in this study.

Strain name	Abbreviation	Description
Staphylococcus aureus	SA	Wild type
Methicillin-resistance*Staphylococcus aureus*	MRSA (ATC32200)	Methicillin resistance *Staphylococcus aureus.*
Accessory gene regulator A	Δ*agr*A gene	NE1532 4 P16 *agr*A SAUSA300_1992
Accessory gene regulator C	Δ*agr*C gene	NE873B17*agr*C, AUSA300_1991

QQ3, 24 mg dissolved in 10 ml Milli-Q water given a concentration of 2.4 mg/ml. Then The amounts of G5 PAMAM dendrimers and QQ3 were calculated and added to the reaction mixture, with continuous stirring for 24 h in the dark at 4 °C. Then the complex was stored at (– 30) for further use.

2.4. Characterization of G5 complex

The vesicles size and polydispersity index (PDI) were determined for the complex and blank PAMAM dendrimer G5, using the Zeta sizer Nano ZS (Malvern Instruments, UK). Dilution 1:5 ratio in Milli-Q water for the formulation was used and the zeta potential was also measured by Zeta sizer Nano ZS (Malvern Instruments, UK).

2.5. Transmission electron microscopy (TEM)

The blank of PAMAM dendrimer G5 and G5 complexes were visualized using Transmission Electron Microscopy (TEM) in order to evaluate the size and morphology.

2.6. Determination of drug encapsulation efficiency (EE%)

In-direct method was carried out using dialysis membrane. The G5-QQ3 complexes was placed into a cellulose membrane with MWCO 12000 Da, then immersed in deionized water and stirred for 1 h at 4 °C. After that, 1 ml of from the media was withdrawn and analysis by HPLC-UV. EE% was calculated by the following equation:

$$\%\text{Entrapment Efficiency} = \frac{\text{total amount of drug loaded} - \text{free drug}}{\text{total amount of drug loaded}} \times 100$$

2.7. Instrumentation and chromatographic conditions

The analysis of the QQ3 peptide was performed at Jazeera Pharmaceutical Industries Ltd. (Riyadh,Saudi Arabia). The method for analysis was conducted according to the company reference sheet for analysis of the QQ3 peptide. The separation was carried out at 25 °C, using column Luna 5U (C18, 150x4.6, 3 µm) and the mobile phase was a linear gradient of a mixture of water and acetonitrile, both containing 0.1% (v/v) TFA, at a flow rate of 0.5 ml/min, the injection volume was 20 µl, wavelength 214 nm and the run time was 10 min. The mobile phase solutions were degassed using a sonicator and filtered through a 0.45 µm filter and the software utilized for data analysis was BREEZE (version 2).

2.8. In vitro release of the QQ3-G5 complex

Briefly; about 200 µl of G5-QQ3 complex were taken in a dialysis cellulose membrane with a molecular weight MWCO12000Da. The dialysis bag was then immersed into a beaker containing 20 ml of phosphate buffer saline (pH 7.4). The beaker was continuously shaken in a thermostat (37C). Around 500 µl of each sample was collected at specific time points for 4 days and replaced every time with phosphate buffer saline. The samples were analyzed by HPLC, and the percent of

drug released was calculated at each time interval and plotted against time. The methods were conducted in triplicate.

2.9. Determination of minimum inhibitory concentration (MIC) on bacterial growth

The concentrations of G5-QQ3 complex and blank G5 that was able to inhibit the growth of 50 % of bacterial strains were determined using the bioscreen C system. Overnight culture of all bacterial strains was adjusted to an OD 0.08–0.1, then 200 µl of bacterial broth was added to 96 well plates. The plates were placed in Bioscreen C reader and the optical density of bacterial growth was recorded for 24 h at wavelength 600 nm.

2.10. Biofilm inhibition assay

Crystal violet assay (CV) staining was used to assess the effect of the MIC50 of the formulated nanoparticles and blank G5 against all bacterial strains' biofilm formation. The overnight culture was adjusted to an OD600- 0.08–0.1, and then 100 µl of bacterial broth suspension was inoculated in a 96-well microtiter sterile plate, containing 100 µl of G5-QQ3 complex. The plate was incubated at 37 °C with continuous shaking at 150 rpm overnight. Planktonic cells were removed and the wells were washed twice time with 0.9% NaCl and inverted to dry at room temperature for 1 h, then 0.1% (v/v) crystal violet was added to the wells for bacterial staining for 15 min. The excess stain was removed and washed 3 times with 0.9% NaCl, etha-nol-acetone (80:20 v/v) was added to solubilized bound crystal violet. The absorbance of stained bacteria was measured by an Elisa Plate reader.

2.11. Biofilm eradication test

The overnight culture of all strains was adjusted to OD600 0.1. After that, 150 µl of the suspension will be added to each of the 96-well microtiter plates and incubated at 37 °C for 24 h to allow biofilm formation. The biofilm formation was confirmed, by the presence of microparticles at the bottom of the wells, any planktonic bacterial cells were removed. The plate was washed twice with PBS, and the formulated nanoparticles and blank G5 at MIC50 were added to the 96-well plate and incubated at 37 °C for 24 h. After that, the compounds were removed, and the wells were rinsed twice with PBS and then stained with 10% crystal violet followed by incubation at 25 °C for 5 min. The crystal violet was discarded and solubilized by adding ethanol-acetone (80:20 v/v) at 25 °C for 15 min, then transferred to a new 96-well plate. Then the OD600 was measured by a plate reader.

2.12. Hemolytic activity analysis

Overnight cultures of bacterial strains were diluted to an OD 600-0.08-0.1, then a small amount of the broth suspension was mixed with G5-QQ3 complex, and blank, G5 and spotted on to blood agar and incubated overnight at 37 °C for 24 and 48 h. The hemolytic activity was observed on plates as transparency around the colonies.

2.13. Confocal microscopy

Overnight culture of all bacterial strains was treated with MIC50 of the QQ3-G5 complex and with the blank G5. The effect of formulated nanoparticles on bacterial cell viability was investigated by confocal laser scanning microscope, with a Live/Dead® BacLight™ viability kit containing a universal stain SYTO 9 and propidium iodide (PI). Cell images were acquired using the Leica Application Suite Adced Fluorescence software, with a magnification power of 40× using an oil-immersion objective lens. An argon-based laser was applied for excitation at 488 nm, and HeNe laser for excitation at 543 nm. The SYTO 9 and PI emission were set at 528 nm and 645 nm respectively. By sequential scanning, the images were obtained and processed in Image J software.

2.14. Scanning electron microscopy (SEM)

To visualize biofilm formation, all bacterial strains were grown overnight in TSB at 37 °C. Then the cultures were adjusted to OD 600-0.08-0.1. Then Polyvinyl (Fisher Scientific) coverslips were placed in each well of a Thomas 6-well plate before being filled with 2 ml of TSB medium and 2 ml of diluted culture. Biofilms were formed on the coverslips at 37 °C for 24 h. The samples were fixed with 3% glutaraldehyde in phosphate buffer pH 7.2 for 24 h, and washed 3 times, the samples were postfixed for 1 h with 1% osmium tetroxide (in H2O). Then applied in to an ethanol dehydration series of 50, 60, 70, 80, 90, and 2 × 100% (v/v) ethanol, for 5 min at each concentration. The samples were dried for 1 day and sputter-coated with a palladium-gold film. The produced biofilm was viewed with a SEM/EDS system in a high-vacuum mode at 20 kV.

2.15. Cytotoxicity MTT assay

Macrophage RAW 264.7 cells were obtained from the American Type Culture Collection (ATCC). The cells were cultured in DMEM media with 10% fetal bovine serum, 1% penicillin, and 1% streptomycin and incubated with 5% carbon dioxide at 37 °C. RAW 264.7 (5×10^3 cells/well) cells were cultured overnight in 96-well plates and different concentrations (10–80 µM) of loaded nanoparticles and blank were added. The plates were allowed to continue incubation for 48 h. Finally, the cell viability was determined by kit I (MTT) assay. Absorbance at 570 nm was documented by a microplate reader.

3. Results

3.1. Particles size and ζ-potential

The Zetasizer was utilized to determine the particle size of the blank G5 and the QQ3 peptide-loaded G5. The results indicated that the particle size of the blank G5 was 153 nm, while the particle size of the QQ3 peptide-loaded G5 increased to 276 nm. It is noteworthy that the particle size of the QQ3 peptide-loaded G5 remained within the nanosized range, which is defined as <500 nm. The PDI value was also evaluated for both the blank dendrimer and the loaded dendrimer. The results indicated that there was no significant change in PDI between the loaded PDI value of 0.33 and the blank dendrimer PDI value of 0.2 ($p < 0.05$). Furthermore, the ζ-potential measurements were conducted for the blank G5, which yielded a value of −0.56 mV. Upon loading with the QQ3 peptide, the dendrimer acquired a negative charge, resulting in an ζ-potential of −13 mV (Table 2).

3.2. TEM images of QQ3-G5 complex and blank G5 treated bacterial biofilms

The morphology of the particles was analyzed through the utilization of Transmission Electron Microscopy (TEM), and the outcomes are presented in Fig. 2. It was observed that both the nanoparticles in the G5-QQ3 complex and the blank G5 exhibited a nearly spherical shape, with the blank nanoparticles displaying this characteristic more prominently. The size of the loaded nanoparticles was approximately 263 nm, while the blank G5 nanoparticles measured around 167 nm. The

Table 2
The particles size and ζ-potential.

Average	G5-QQ3 complex	G5
Z average diameter (nm) ± SD	276 nm ± 9.2	160.1 nm ± 8.9
Polydispersity Index (PDI) ± SD	0.33 ± 0.008	0.22 ± 0.005
Zeta potential (Mv) ± SD	−14 mV ± 1.05	−0.56 mV ± 1.04

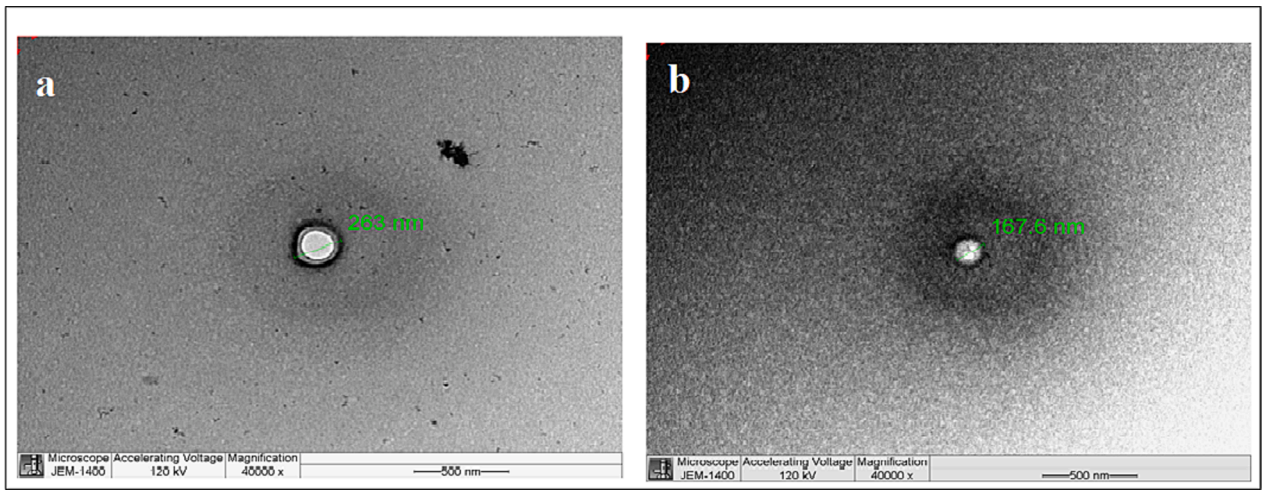

Fig. 2. TEM images: (a) G5 loaded with QQ3 and; (b) Blank G5.

observed increase in particle size provides confirmation of the successful loading of the peptide.

3.3. Encapsulation efficacy

The quantitative analysis of the G5-QQ3 complex to determine the encapsulation efficacy (EE%) was obtained from HPLC showed a high percent of encapsulation efficiency equal to 98%.

3.4. In vitro drug release

The present study investigated the release profile of the QQ3-G5 complex in a 30 ml phosphate buffer solution at pH 7.4 over a period of 96 h. The release samples of the QQ3 peptide were analyzed using high-performance liquid chromatography (HPLC). The experimental setup involved the use of a cellulose dialysis tube that was sealed at both ends. The results were obtained by plotting the release percentage of the nanoparticles against time, and it was observed that the release was sustained and gradually increased over time, as depicted in Fig. 3. The release profile was characterized by a sustained flow manner and the percentage release of the peptide from dendrimer over 72 h was 80%. During the initial 10-hour period, it was observed that approximately 40% of the peptide had been liberated. This phenomenon can be attributed to the presence of weak forces that retained a portion of the peptide within the dendrimer structure. Subsequently, the majority of peptide release took place between the 40th and 72nd hour. This can be attributed to the fact that the remaining peptides were probably encapsulated within the dendrimer matrix, necessitating a longer duration for their release.

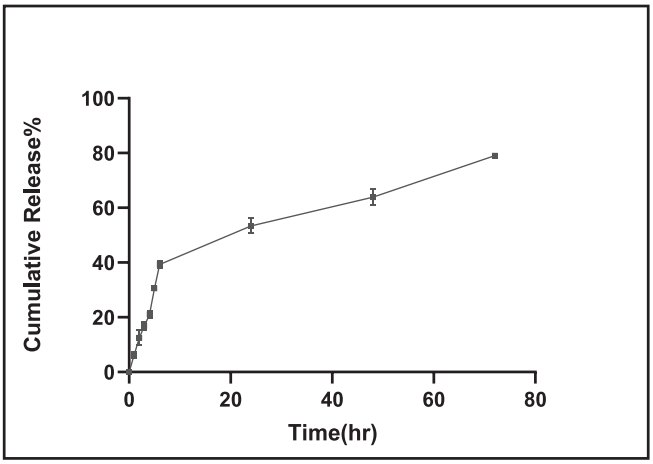

Fig. 3. *In-vitro* release profile of QQ3-G5 complex. (mean ± SD, n = 3) ($p < 0.05$).

3.5. The minimum inhibitory concentration (MIC) on bacterial growth

QQ3-G5 complex and blank G5 were tested against all bacterial strains and Vancomycin was used as a positive control. The selected concentrations of the nanoparticles ranged from 3 μM to 80 μM as shown in Fig. 4, and the MIC_{50} for all strains is listed in Table 3. By adding the QQ3-G5 complex the growth of all strains was reduced as the concentration increased and the MIC_{50} was determined based on the inhibition of the growth of 50% of MRSA, *S.aureus*, *agr*A, and *agr*C population. QQ3 peptide was tested against MRSA and inhibition of growth was observed at a concentration of 100 μM. The MIC_{50} was 18 μM for MRSA, and 15 μM for *S.aureus*, *agr*A, and *agr*C. All experiments were performed as triplicate and $p < 0.05$.

3.6. Biofilm inhibition assay

Upon exposure to the MIC_{50} of the G5-QQ3 complex, the cells exhibited a notable inhibition of biofilm formation across all strains. The findings indicate that MRSA and *S.aureus* experienced a 60% and 63% reduction in biofilm formation, respectively, while *agr*A and *agr*C mutants exhibited a 68% and 70% reduction in biofilm formation respectively. The G5 blank also exhibited an inhibitory effect on biofilm formation, with reductions of 39%, 45%, and 50% observed for MRSA, *S. aureus*, and *agr* mutants, respectively. The biofilm reduction achieved by the G5-QQ3 complex was statistically significant ($p < 0.05$), as illustrated in Fig. 5.

3.7. The antibiofilm efficacy of the QQ3-G5 complex

As depicted in Fig. 8, the application of the MIC_{50} of the G5-QQ3 complex resulted in the elimination of over 50% of the pre-formed biofilm. The biofilm reduction percentages were found to be 63%, 73%, 72%, and 75% for MRSA, *S.aureus*, *agr*A, and *agr*C, respectively. Conversely, the use of blank G5 led to a biofilm reduction of 42%, 53%, 57%, and 55% in MRSA, *S.aureus*, *agr*A mutants, and *agr*C mutants, respectively. Notably, the eradication of biofilm by the G5-QQ3 complex exhibited statistical significance ($p < 0.05$), showen in Fig. 6.

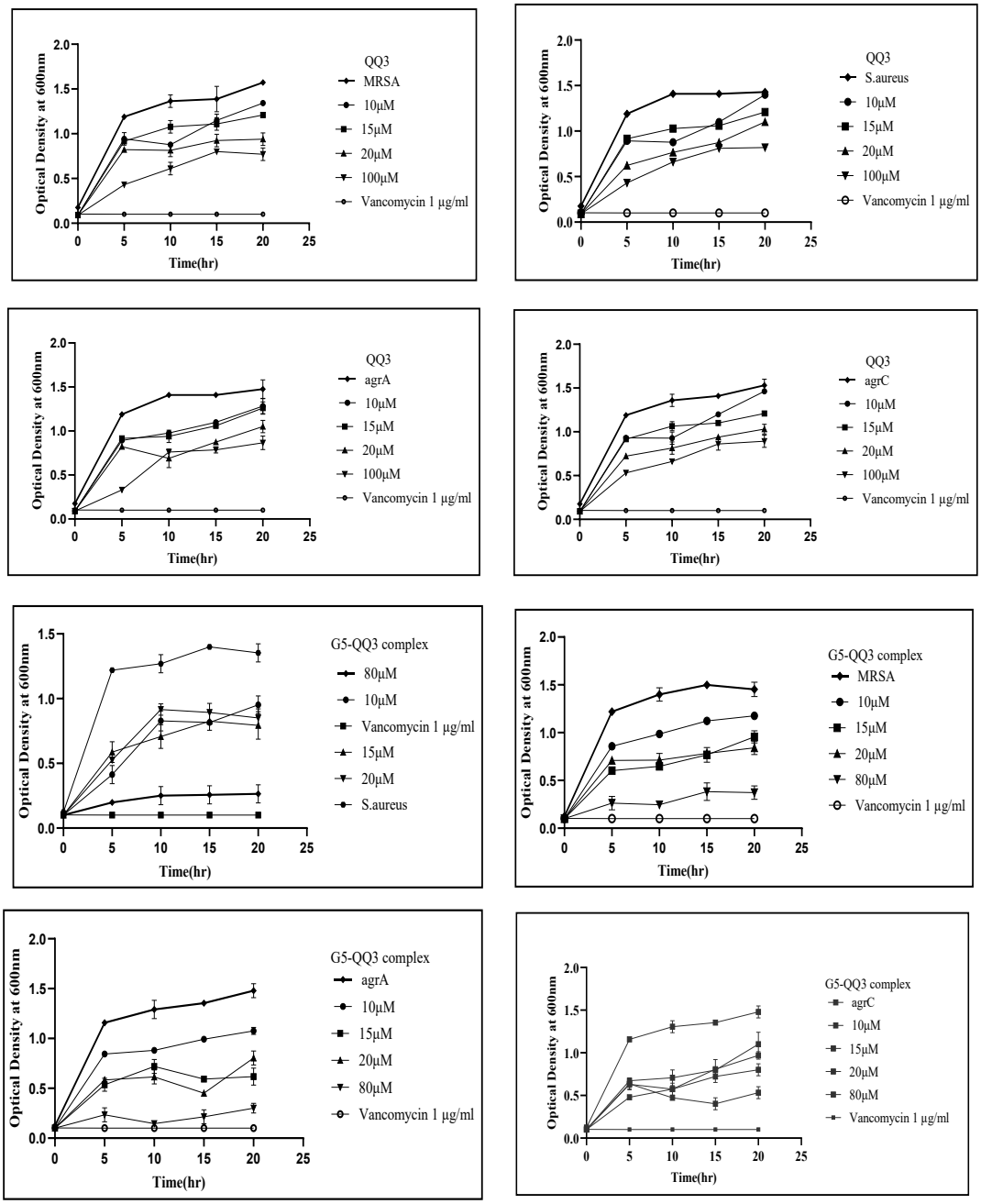

Fig. 4. Growth curves of all strains. (mean ± SD, n = 3) ($p < 0.05$).

3.8. Bacterial viability within formed biofilm after exposure to QQ3-G5 complex by confocal microscopic analysis

Confocal laser scanning microscopy (CLSM) was employed to assess the efficacy of the QQ3-G5 complex and blank G5 in eradicating bacterial strains within the biofilm. Live/dead staining was utilized for all strains. The obtained results are presented in Fig. 9. The untreated alive cells served as the control, and their biofilm structure was visualized in Figs. 7–10. Following treatment with the MIC_{50} of the loaded nanoparticles, the number of dead bacterial cells exhibited a significant increase over a 24-hour period. These findings provide compelling evidence for the bactericidal properties of the QQ3-G5 complex against bacterial cells residing within the biofilm structure.

3.9. SEM images of QQ3-G5 complex and blank G5 treated bacterial biofilms

All strains were visualized under SEM to investigate the morphology of the bacteria in the biofilms before and after treatment with the nanoparticles MIC50. Fig. 11 demonstrates the results; the biofilm of all strains was highly disrupted after treatment with QQ3-G5 complex compared with strains treated with blank G5.

3.10. Hemolysis assay

The inhibitory effects of the G5-QQ3 complex on the hemolysis activity of *S.aureus* and MRSA on blood agar was investigated. The results, as depicted in Fig. 12, revealed that the complex was able to completely inhibit the hemolysis activity of both strains at concentrations of 3, 10,

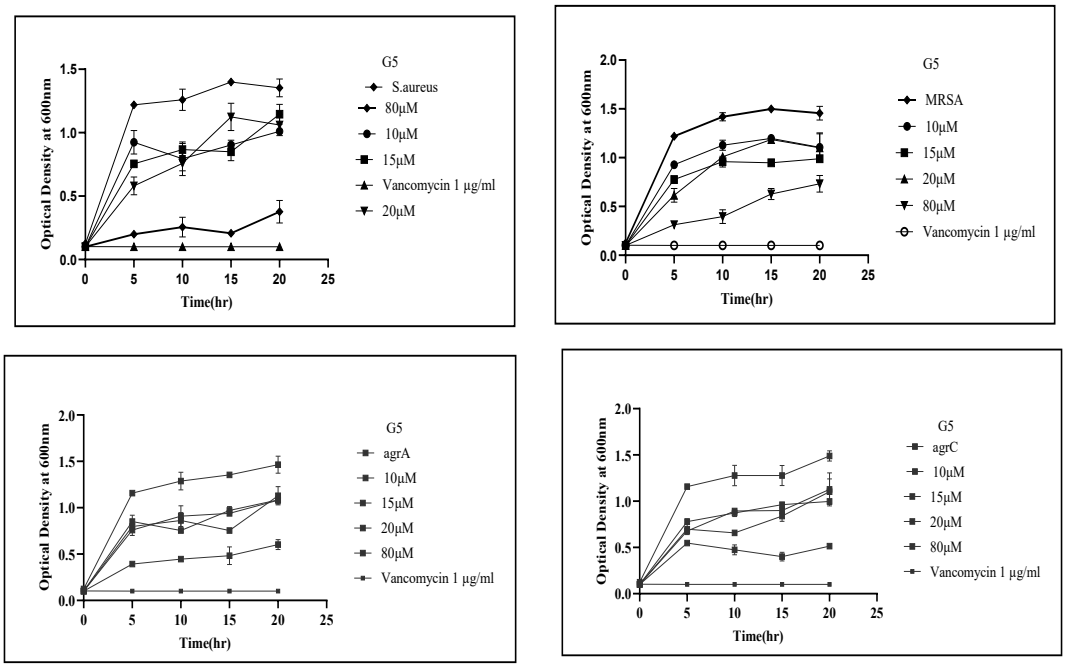

Fig. 4. (*continued*).

Table 3
The MIC_{50} for all strains.

Nanoparticles	MRSA	*S. aureus*	*agr*A,	*agr*C
G5-QQ3 complex MIC_{50} (μM)	18	15	20	20
G5 MIC_{50} (μM)	80	50	80	80
QQ3 MIC_{50} (μM)	100	80	100	100

18, and 20 μM. Specifically, *S.aureus* hemolysis was completely inhibited at a concentration of 3 μM, while MRSA required a higher concentration of 10 μM due to its high resistance. In comparison, the blank G5 exhibited limited effects on hemolysis activity when compared to the loading nanoparticles. Notably, MRSA treated with QQ3 peptide required a high concentration of 100 μM to achieve complete inhibition of hemolysis. These findings confirm the anti-virulence activity of the formulated nanoparticles, as they were able to effectively inhibit the strong virulence activity of both strains at low concentrations.

3.11. In vitro cytotoxicity

Various doses ranging from 3–40 μM, encompassing the MIC_{50} of the QQ3-G5 complex and blank G5, were employed to evaluate their cytotoxicity against the highly sensitive RAW 264.7 cell model. The findings depicted in Fig. 13 indicate that the viability of cells at 3 μM ($p < 0.001$), 10 μM ($p < 0.006$), and 20 μM ($p < 0.007$), which includes the MIC_{50}, remained unaffected in a statistically significant manner.

4. Discussion

MRSA is a predominant pathogen contributing to antimicrobial resistance (AMR) in both community and healthcare settings. Studies have shown that 33% of people carry *S.aureus* in their nose without harm, and two out of every hundred are MRSA carriers (Tiwari et al., 2017). Quorum sensing (QS), is a mechanism that allows cell-to-cell communication due to the population expanding of the bacteria. In *S. aureus* quorum-sensing accessory gene regulator (*agr*) system controls

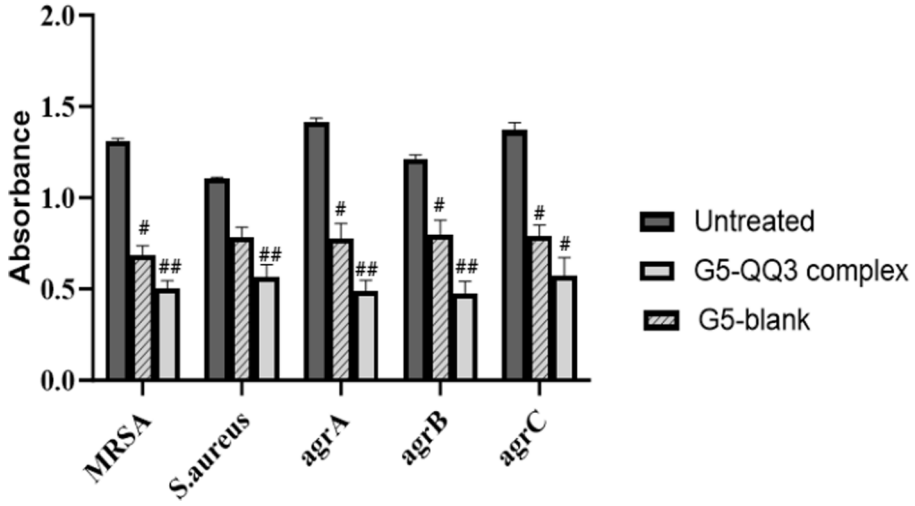

Fig. 5. Inhibition of biofilm formation of MRSA, *S.aureus* and *agr* mutants. (mean ± SD, n = 3) ($p < 0.05$).

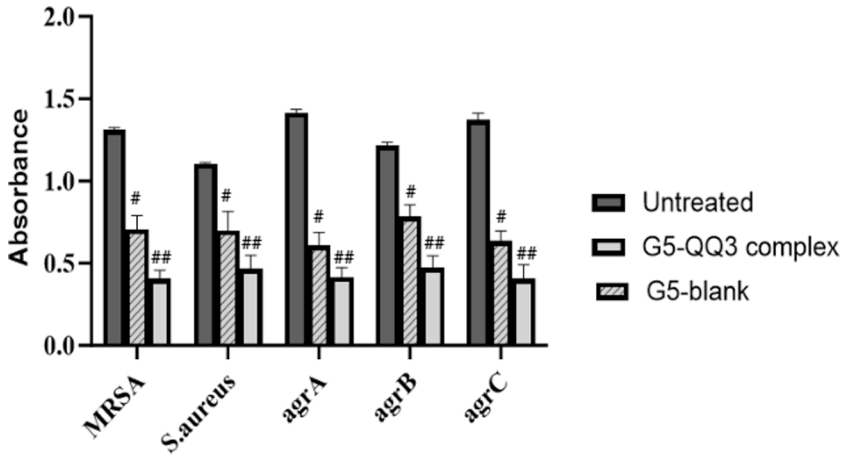

Fig. 6. Eradication of preformed biofilm for all strains by QQ3-G5 complex. (mean ± SD, n = 3) ($p < 0.05$).

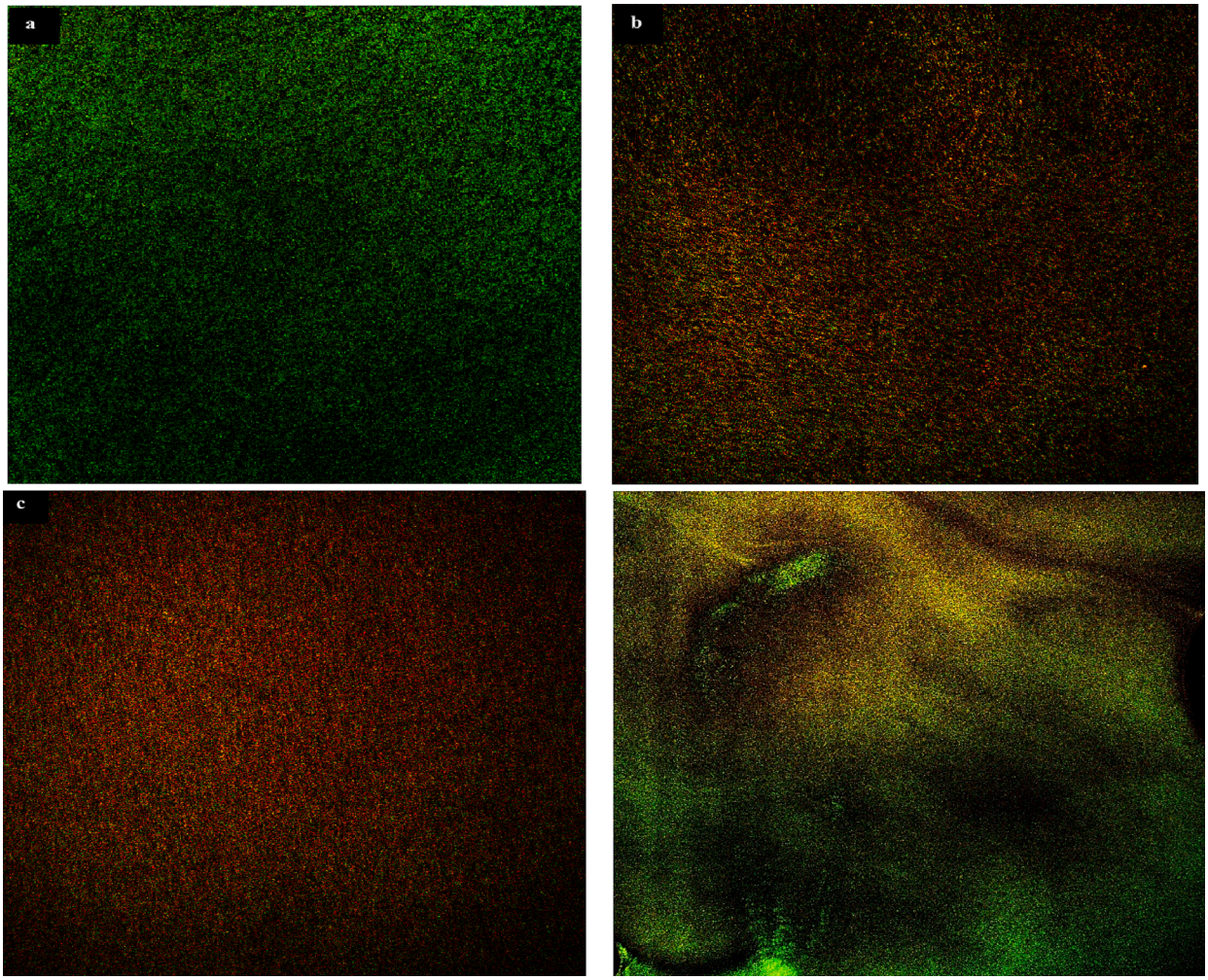

Fig. 7. Live/dead assay. the viability of mrsa after exposure to g5-qq3 complex and blank g5. a) control group in absence of loaded nanoparticles, b-c) mrsa treated with g5-qq3 complex within 24 h, d) MRSA treated with blank G5. results showed a change in cell viability overtime, as an evidenced by the appearance of the red/yellow color that indicate dead cells.

the virulence factors production. In many diseases, the pathogenicity is multifactorial, making it difficult to determine the precise role of each of these factors. Previous studies have found that mutation in the *agr* locus leads to a lack of expression of bacterial virulence factors. Targeting the QS with HK inhibitor will reduce the virulence in resistance strains such as P. aeruginosa (Aleanizy et al., 2020). A study identifies small molecules as HK inhibitors and test them against MRSA. the result showed that these molecules can inhibit different HKs in vitro with antibacterial activity (Huang et al., 2020). Recent studies found that cell-penetrating peptides (CPPs) and antimicrobial peptides (AMPs) have anti-microbial

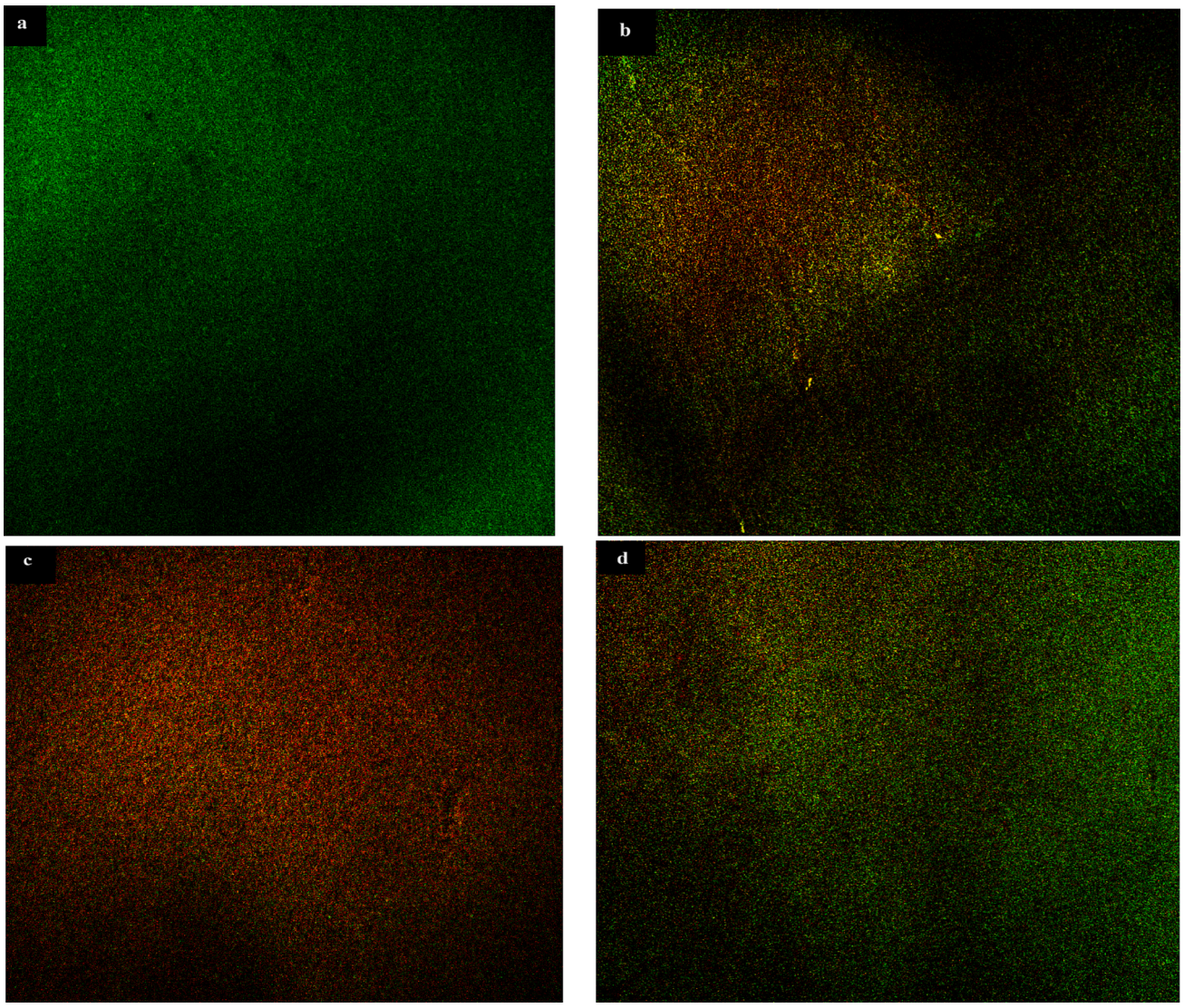

Fig. 8. Live/dead assay. the viability of *S.aureus* after exposure to G5-QQ3 complex and blank G5. (a) Control group in absence of loaded nanoparticles, (b-c) *s.aureus* treated with G5-QQ3 complex within 24 h, (d) *S. aureus* treated with blank G5. Results showed a change in cell viability overtime, as an evidenced by the appearance of the red/yellow color that indicate dead cells.

activity and can eradicate bacterial biofilm more efficiently compared to conventional antibiotics (Falanga et al., 2021).

A previous study hypothesized that some of the quorum-quenching (QQ) peptides were able to reduce the amount of the AIP secretion in WT *S.aureus* compared with mutant *agr*C. The study concludes that QQ peptides work by altering the kinase activity by binding to the *agr*C sensor domain and can inhibit the hemolysis activity in WT *S.aureus* (Xie et al., 2020).

Furthermore, QQ3 peptides used in this study are structurally different from the native AIP, and are larger macrocycles, having thioether linkage instead of thiolactone and no sequence similarity between them. This thioether group stabilizes the QQ3 peptides and prevents the post-translation modification that may occur. Different peptides having divergent primary structures have been tested on *S.aureus* and found that any alteration in the *agr*C ligand will inhibit the *agr* response. The inhibition may occur by noncovalent binding interaction that excludes the AIP from its receptor-binding pocket (Fihn and Carlson, 2021).

Antimicrobial peptides are emerging because of their bioactive property, target affinity, and high potency. The exact mechanism of action of this antimicrobial peptide is elusive and not fully understood. The suggested mechanism includes the peptide may induce complete or partial cell membrane lysis resulting in cell death, or it may cross the membrane and act on intracellular substances (De Alteriis et al., 2018).

This study used PAMAM G5 to have carbomethoxy- pyrrolidone terminated. These dendrimers are water-soluble, biocompatible molecules with highly branched structures that provide many surface areas that can be reactive to microorganisms. The biocompatibility and no immunogenicity are critical for using the dendritic structure. The cationic surface is commonly associated with toxicity. When modifying the surface with carbomethoxy- pyrrolidone moieties the PAMAM dendrimer acquired the biocompatibility features. This modification inhibits the activation of proinflammatory human monocytes with reduced toxicity (Janaszewska et al., 2019). Also, studies use the PAMAM dendrimers to encapsulate silver and it showed a strong antimicrobial activity against gram-positive organisms. PAMAM biocidal activity against *S.aureus* contributed to membrane destruction, and the release of cytoplasmic contents was observed. The particles' morphology was determined using TEM. The nanoparticles for G5-QQ3 complex, and blank G5 were observed (Fig. 3) to have an almost spherical shape, especially in the blank nanoparticles, and a size of approximately 276 nm for the loaded nanoparticles and blank G5 was 160 nm respectively. The difference in size between the blank and

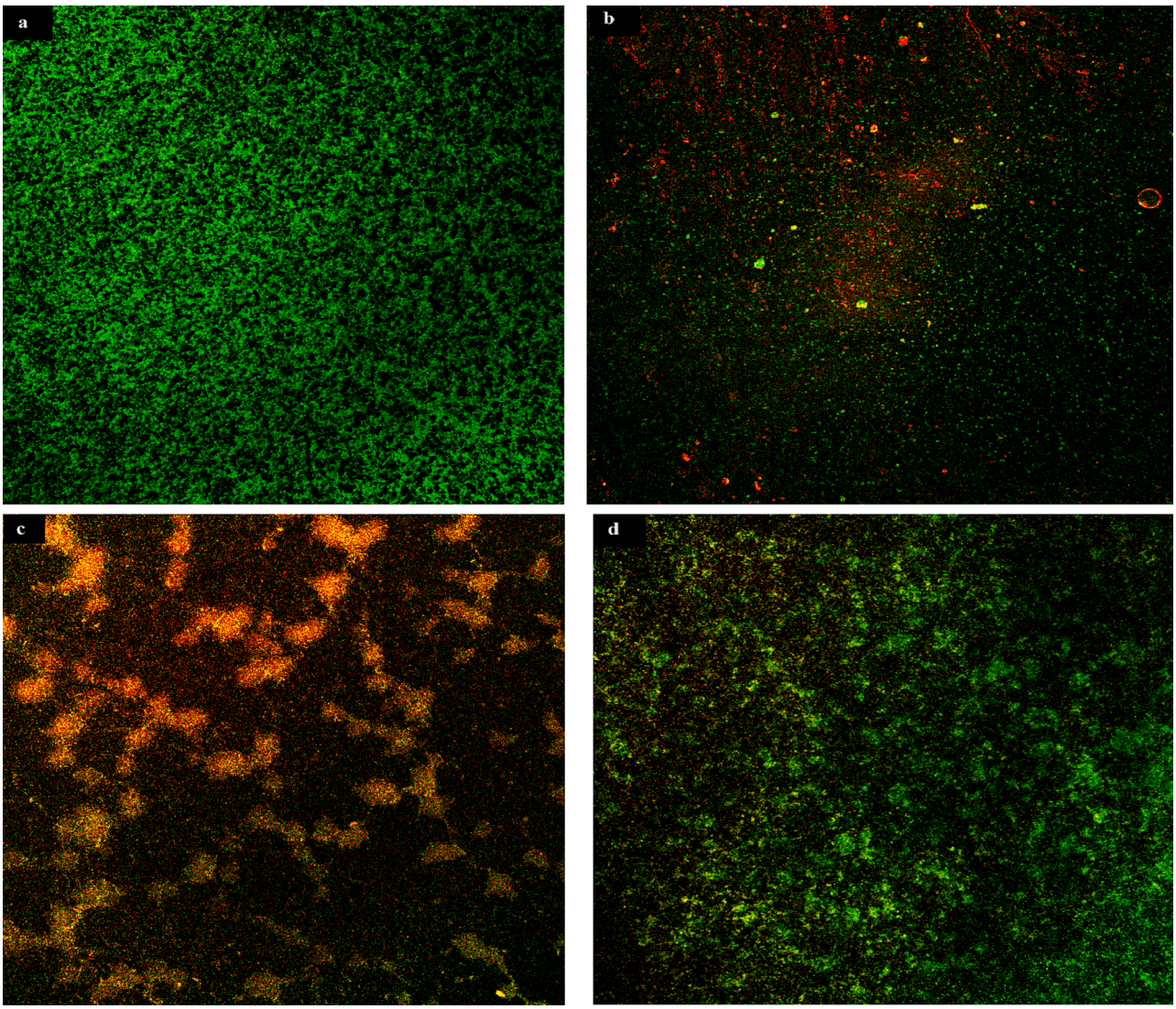

Fig. 9. Live/dead assay. the viability of *agr*A after exposure to G5-QQ3 complex and blank G5. (a) Control group in absence of loaded nanoparticles, (b-c) *agr*A treated with G5-QQ3 complex within 24 h, (d) *agr*A treated with blank G5. Results showed a change in cell viability overtime, as an evidenced by the appearance of the red/yellow color that indicate dead cells.

loaded nanoparticles proves that the loading of the drug was successful. The zeta potential for blank G5 was −0.56 mV. The negative charge was increased upon loading the peptide which has a negative charge to reach −14 mV for the G5-QQ3 complex (Table 1).

Moreover, one of the most potent virulence factors that MRSA uses is the secretion of toxins (α, β, γ, δ) which facilitate spreading, cause tissue damage, nutrient uptake, and make pores in the membrane, leading to the efflux of essential molecules and metabolites. Reducing or inhibiting these hemolysins will reduce the severity of infection and delay the development of biofilms (Aygül and Şerbetçi, 2020).

The hemolytic activity of *S.aureus* and MRSA was tested (Fig. 11). In a previous study (Xie et al., 2020). the hemolysis activity of *S.aureus* was inhibited with QQ3 peptide at a concentration of 10 μM and the effect of QQ3 on MRSA has never been tested. In this study, the QQ3 peptide was able to inhibit the hemolytic activity of MRSA at a concentration of 100 μM. When loading the peptide on PAMAM G5 dendrimer the inhibitory concentration was reduced for both *S.aureus* and MRSA to 3 μM and 10 μM respectively. Blank G5 limited the hemolysis activity but did not inhibit it completely compared with loaded nanoparticles. This result confirms that the G5-QQ3 complex has a potent anti-virulence action and both produce a synergism effect. The bacterial growth curve of all strains (Fig. 6) showed that the QQ3-G5 complex inhibits the bacterial growth of *S.aureus* wild type, MRSA, *agr*A mutant, and *agr*C mutant at MIC50 18 μM. Whereas, blank G 5 only reduces the rate of growth at 80 μM. MRSA treated with naked QQ3 peptide showed an inhibition of growth with a high concentration of 100 μM. This result confirms that PAMAM G5 dendrimer is important for encapsulating the peptide and preventing its uptake by the bacterial cells, and suggesting a synergism effect. When treating MRSA with G5-QQ3 complex a lower concentration (18 μM) was required to inhibit the growth of the strain, compared with 100 μM and 80 μM for the QQ3 peptide and G5 blank respectively. By blocking hemolysin expression, and inhibiting bacterial growth in all strains, these results confirm the potent anti-virulence and antimicrobial properties of nanoparticles complex and suggest a synergism effect. The biofilm formation is one of the most potent virulence factors that *S. aureus*, and MRSA phenotype use to resist antibiotics. In prosthetic implants, *agr* mutants are frequently isolated. Bacteria within biofilms can be up to 1000 times more resistant to antibiotics than plank-tonic cells. The *agr* system regulates the switch between planktonic and biofilm lifestyles and has a crucial role in biofilm development. Findings from antibiofilm assay, SEM image, and live\dead viability assay, shown in Figs. 8, 9, and 10, all together confirm that QQ3-G5 complex was able to inhibit, penetrate, and eradicate the biofilm in all strains; *S. aureus*, MRSA, *agr*A mutant, and *agr*C mutant, and kill all strains within the

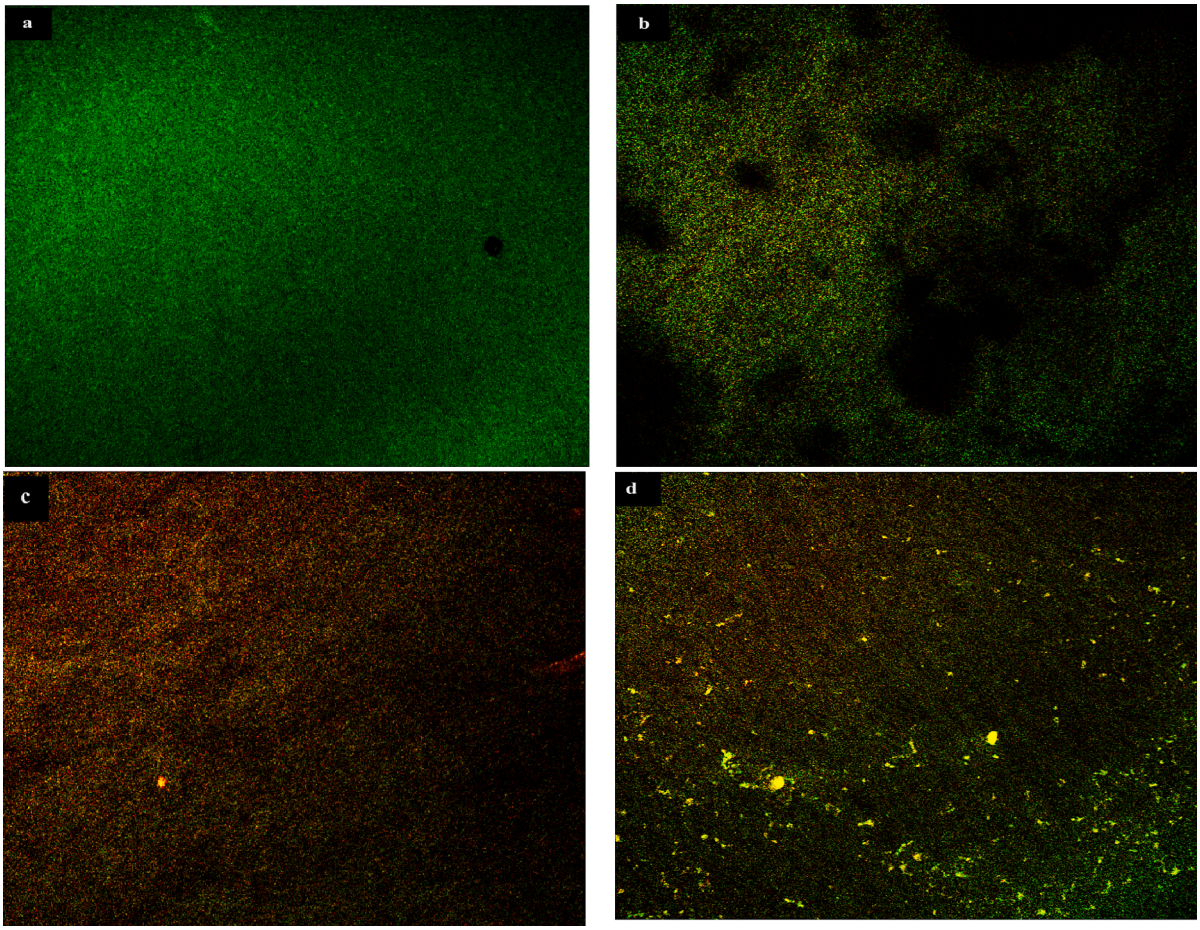

Fig. 10. Live/dead assay. The viability of *agr*c after exposure to G5-QQ3 complex and blank G5. (a) Control group in absence of loaded nanoparticles, (b-c) *agr*c treated with G5-QQ3 complex within 24 h, (d) *agr*c treated with blank G5. results showed a change in cell viability overtime, as an evidenced by the appearance of the red/yellow color that indicate dead cells.

biofilm structure.

The percentage of biofilm inhibition ranges from 58 to 70%, and the percentage of eradication ranges from 63 to 75%. QQ3-G5 complex has an excellent potential to eliminate mature biofilm as it was able to diffuse through the poly-saccharide matrix and destabilize it, due to its antimicrobial action. This result proves the potent antibacterial and anti-virulence actions of the formulated nanoparticles. Also, suggesting that the QQ3-G5 complex not only works as an inhibitor for *agr* C, as it inhibits the biofilm formation and growth of the *agr*C mutant strain, but it may also target another component in the *agr* system, or disrupt cell membrane. As noted earlier the phosphorylation of *agr* A is catalyzed by *agr* C and both form the TCS, using inhibitors for *agr*C or *agr*A will be efficient antagonists of the *agr* system. Some *S.aureus* strains I311T and F264C acquire *agr*C mutation naturally and these were associated with delayed and reduced AIP production without abolishing the activity. Also, an induced point mutation in *agr*C in ST22 and ST239 in *S.aureus* strains caused a delay in AIP production, but it responded to exogenous AIP. Thus, the *agr* system is complex and controlled by numerous regulators, inhibitors, and other factors protein. The activity of these alternative factors may be responsible for the sensitivity to the exogenous *agr*C ligand, but the underlying mechanism is not clear. Also, it was reported that using AIPs from other staphylococcal species can down-regulate the function of the *agr* system. Some peptides have a district structure from native AIP and may act as an allosteric inhibitor of *agr*C (Sloan et al., 2019). RAW 264.7 cells were used to investigate the cytotoxicity effect of the formulated nanoparticles. This cell line is an appropriate model of macrophages and is considered a very sensitive cell line. MRSA can survive within the phagocytes and this intracellular stage is important for persistence, dissemination, and infection (Zhai et al., 2017). The QQ3-G5 complex and blank G5 were tested against RAW 264.7 cells and the result showed that the cytotoxicity of the nanoparticles is dose-dependent. The concentration which includes the MIC50 10 μM, 20 μM was cytocompatible and the reduction in viability was not significant. PA-MAM dendrimers have a generation-dependent cytotoxicity and it is related to the number of surface amino groups, it causes depletion of intracellular glutathione and fast apoptosis (Galanakou et al., 2023).

In this study, PAMAM G5 loaded with HK inhibitor peptide QQ3 resulted in antimicrobial action against a highly resistance strain MRSA, *S. aureus* WT, and QS mutant. The QQ3 peptide was encapsulated by the PAMAM G5, this protects the peptide to produce its action by either competitive binding to the sensor HK *agr*C, thus preventing AIP-agrC interaction and disrupting the agr system. Other proposed mechanism includes; targeting other inter-cellular component or disrupting cell membrane. Both actions led to inhibiting important virulence factor production in *S. aureus* and MRSA phenotype. Furthermore, the study suggests that PAMAM G5 and QQ3 produce a synergistic effect as both have antimicrobial action that was evaluated with different in-vitro methods on different strains; *S. aureus* and MRSA and QS mutant. The synergistic effects of this complex were examined on planktonic bacterial cells, and their efficacy on biofilm inhibition was tested. The formulated nanoparticles showed a cytocompatible feature when tested against RAW 264.7 cells. Anti-virulence drug development are attractive target and the chance of resistance to this therapy is low as the antimicrobial does not threaten the survival of the microbe. Using anti-virulence with antibiotics as co-treatment appears to have great

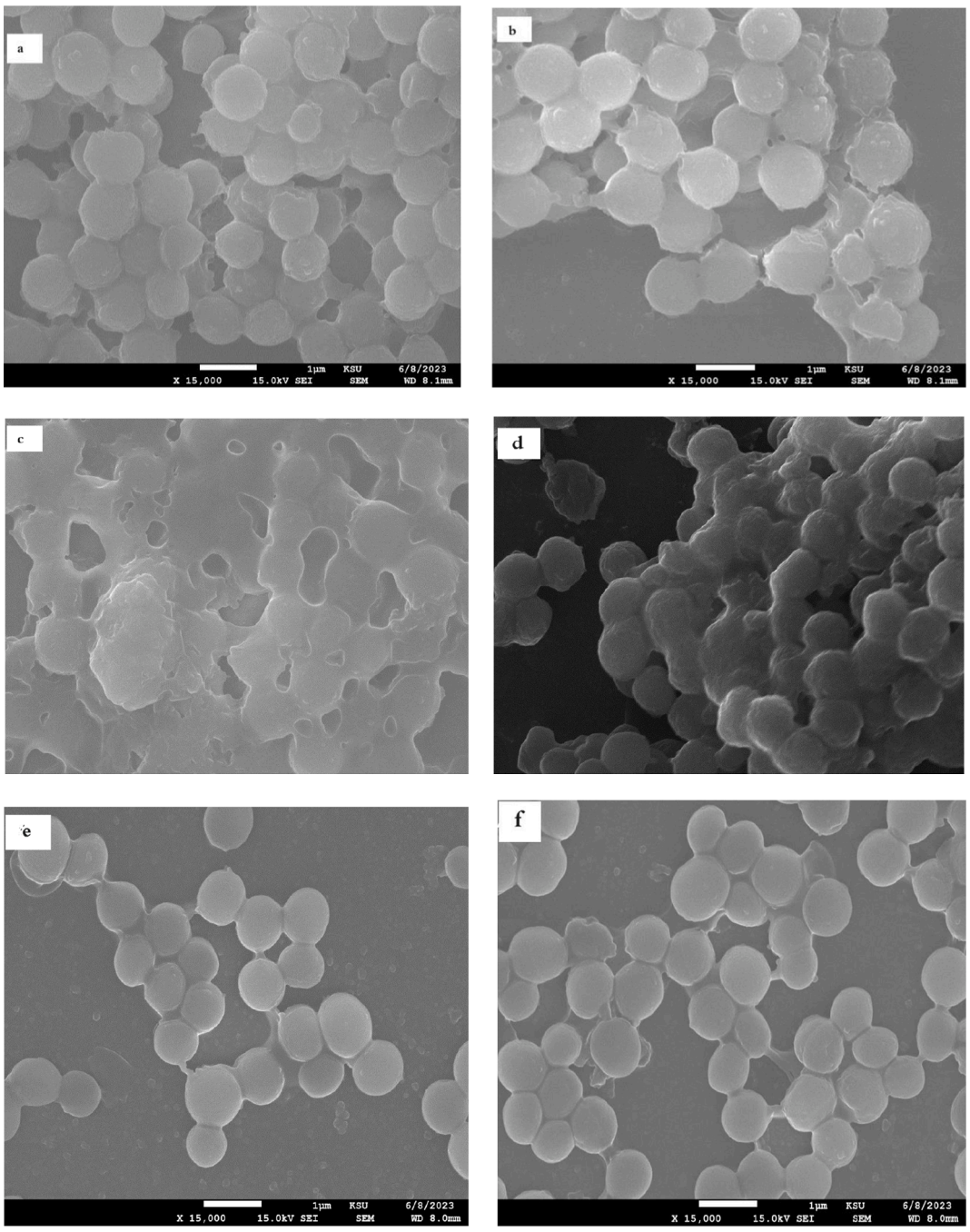

Fig. 11. Scanning electron microscopy (SEM) images of (a) Untreated *S.aureus*, the biofilm is shown as dense extracellular matrix around the cells, (b) Untreated MRSA, (c) Untreated *agr* A mutant. (d) Untreated *agr* C mutant. (e, f, g, h) *S.aureus*, MRSA, *agr* A mutant, and *agr* C mutant treated with G5-QQ3 complex.). I, j, k, l) *S. aureus*, MRSA, *agr* A mutant, and *agr* C mutant treated with blank G5.

promise (Calvert et al., 2018).

5. Conclusions

The emergence of antimicrobial resistance among pathogenic bacteria, including MRSA, poses a significant threat to public health. In this study, the G5-QQ3 complex were synthesized, and they exhibited a minimum particle size, maximum encapsulation efficiency, and sustained in vitro release. These nanoparticles demonstrated potent antibacterial and anti-virulence activity against all tested *S.aureus* and MRSA phenotypes. Upon loading the peptide onto PAMAM G5 dendrimer, the inhibitory concentration for both S. aureus and MRSA was decreased to 3 μM and 10 μM, respectively. The formulated nanoparticles effectively reduce the biofilm formation by up to 60% in MRSA and 70% in *S. aureus*. The cytotoxicity of the nanoparticles was evaluated by testing the QQ3-G5 complex and blank G5 against RAW 264.7 cells. The findings indicated that the cytotoxicity of the nanoparticles exhibited a dose-dependent relationship. The results of this study suggest that G5-QQ3 complex hold potential for future therapeutic use in the treatment of MRSA and *S. aureus* infections, as well as in the prevention of biofilm formation.

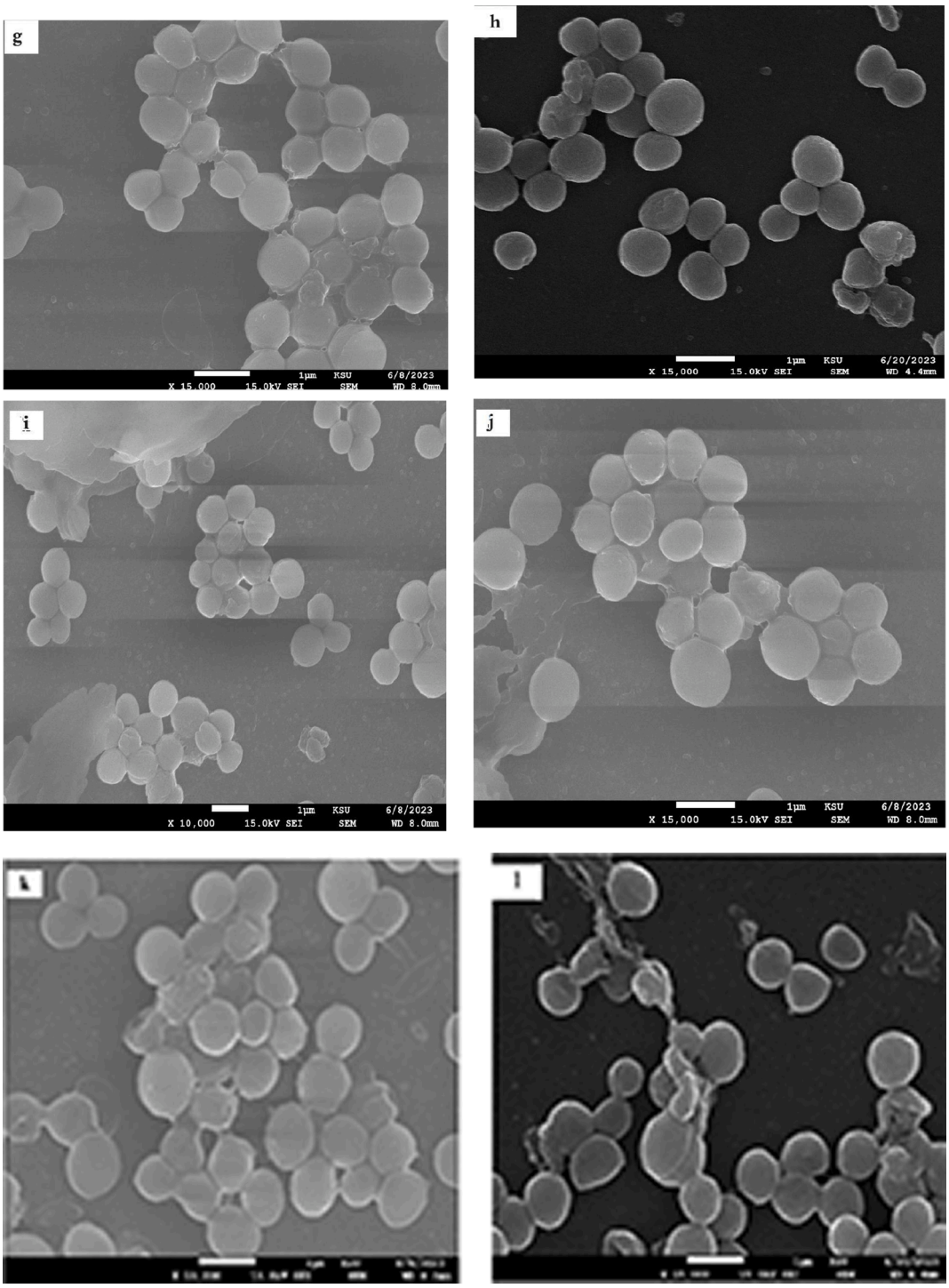

Fig. 11. (*continued*).

Author contributions

FSA, FYA and NAA: Conceptualization, design of study, methodology, acquisition of data, validation, supervision Resources, visualization and writing final draft preparation. NAA: Acquisition of data, analysis of data, visualization, interpretation of data and writing final draft preparation. AAA and MMA: cytotoxicity study, investigation, interpretation of all chemical analysis, and validation. RTA interpretation of data and chemical analysis of nanoparticles. All authors have read and *agr*eed to the published version of the manuscript.

Funding

This research project was supported by the Researchers Supporting Project number (RSP2023340), King Saud University, Riyadh, Saudi Arabia.

Institutional Review Board Statement: Not applicable.

Informed Consent Statement: Not applicable.

CRediT authorship contribution statement

Naifa A. Alenazi: Conceptualization, Methodology, Validation,

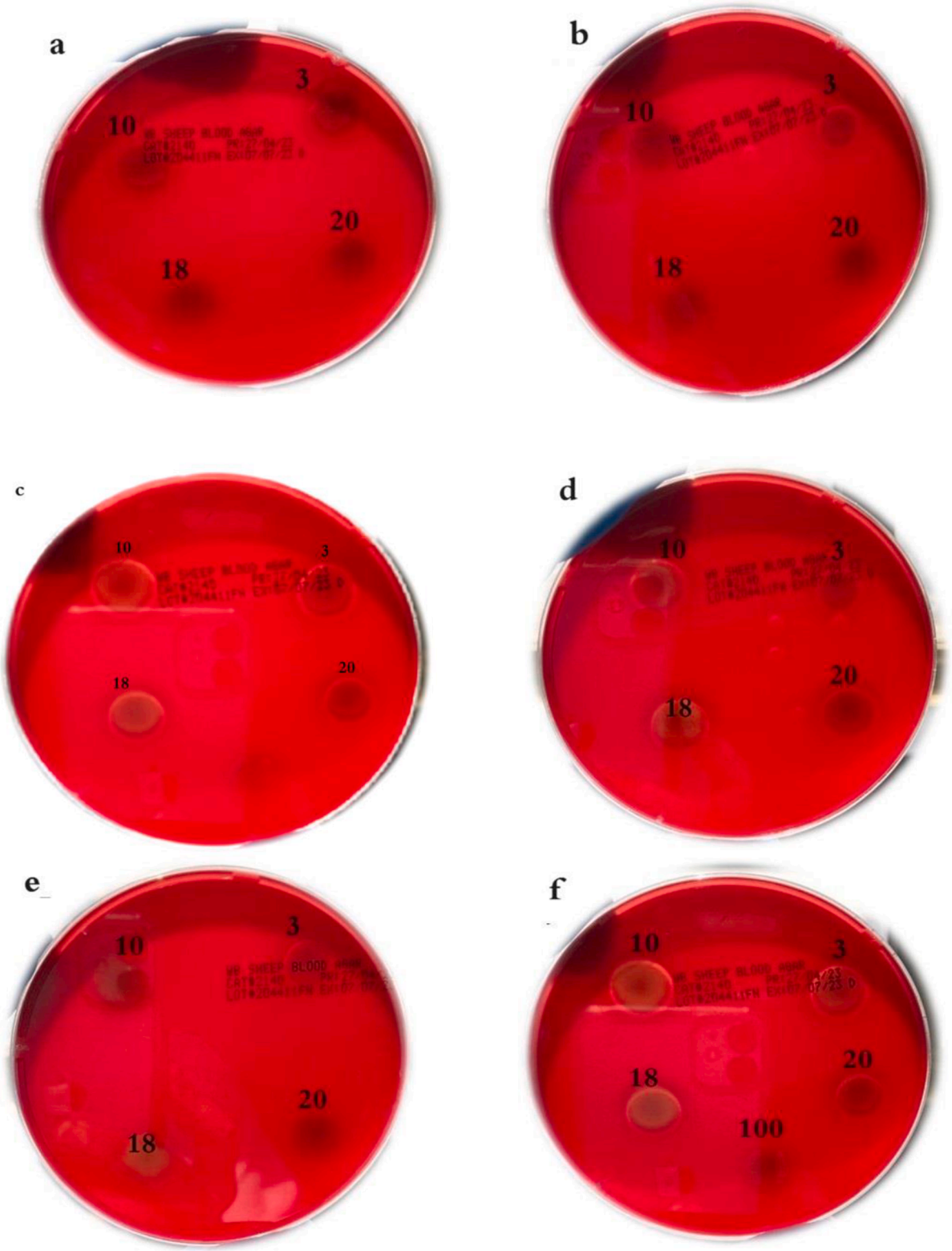

Fig. 12. Hemolysis activity, (a) *S.aureus* treated with G5-QQ3 complex, (b) MRSA treated with G5-QQ3 complex, (c) *S.aureus* treated with blank G5 h) MRSA treated with blank G5, (d) *S.aureus* treated with blank G5 (e) *S.aureus* treated with naked QQ3, hemolysis inhibited at 10 μM, (f) MRSA treated with QQ3 peptide hemolysis inhibited at 100 μM.

Supervision, Resources, Visualization, Visualization. **Fadilah S. Aleanizy:** Conceptualization, Methodology, Validation, Supervision, Resources, Visualization. **Fulwah Y. Alqahtani:** Conceptualization, Methodology, Validation, Supervision, Resources, Visualization. **Abdullah A. Aldossari:** Investigation, Validation. **Mohammed M. Alanazi:** Investigation, Validation. **Rihaf Alfaraj:** .

Declaration of Competing Interest

The authors declare that they have no known competing financial

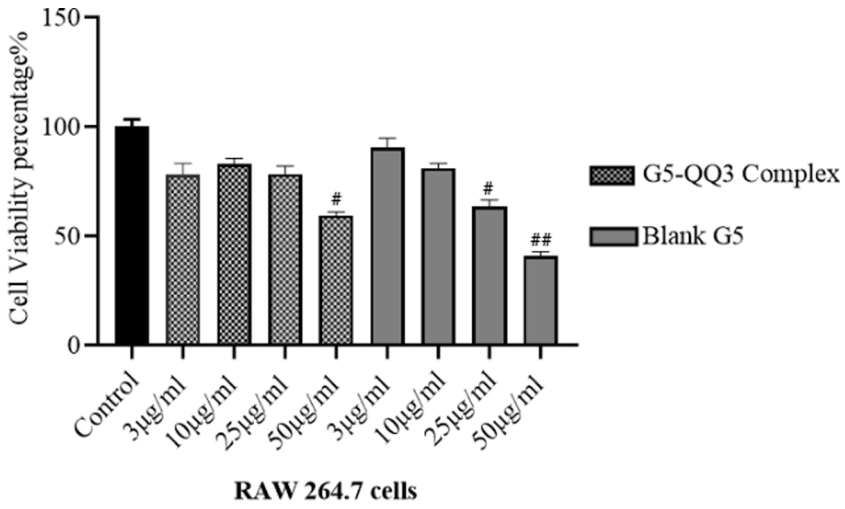

Fig. 13. MTT assay for the QQ3-G5 complex and blank G5. (mean ± SD, n = 3) ($p < 0.05$).

interests or personal relationships that could have appeared to influence the work reported in this paper.

Acknowledgments

The authors would like to thank Deanship of scientific research in King Saud University for funding and supporting this research through the initiative of DSR Graduate Students Research Support (GSR), King Saud University, Riyadh, Saudi Arabia.

References

Al Bshabshe, A., Joseph, M.R., Awad El-Gied, A.A., Fadul, A.N., Chandramoorthy, H.C., Hamid, M.E., 2020. Clinical relevance and antimicrobial profiling of methicillin-resistant Staphylococcus aureus (MRSA) on routine antibiotics and ethanol extract of mango kernel (Mangifera indica L.). BioMed Res. Int.

Aleanizy, F.S., Alqahtani, F.Y., Seto, S., Al Khalil, N., Aleshaiwi, L., Alghamdi, M., Alsarra, I., 2020. Trastuzumab targeted neratinib loaded poly-amidoamine dendrimer nanocapsules for breast cancer therapy. Int. J. Nanomed. 5433–5443.

Aljeldah, M.M., 2020. Prevalence of methicillin-resistant staphylococcus aureus (MRSA) in Saudi Arabia: a systematic review. J. Pure Appl. Microbiol. 14 (1).

Aygül, A., Şerbetçi, T., 2020. The antibacterial and antivirulent potential of Hypericum lydium against *Staphylococcus aureus*: inhibition of growth, biofilm formation, and hemolytic activity. Euro. J. Integ. Med. 35, 101061.

Calvert, M.B., Jumde, V.R., Titz, A., 2018. Pathoblockers or antivirulence drugs as a new option for the treatment of bacterial infections. Beilstein J. Org. Chem. 14 (1), 2607–2617.

Chen, Y., Sun, L., Ba, X., Jiang, S., Zhuang, H., Zhu, F., Yu, Y., 2022. Epidemiology, evolution and cryptic susceptibility of methicillin-resistant *Staphylococcus aureus* in China: a whole-genome-based survey. Clin. Microbiol. Infect. 28 (1), 85–92.

Choudhary, K.S., Mih, N., Monk, J., Kavvas, E., Yurkovich, J.T., Sakoulas, G., Palsson, B. O., 2018. The *Staphylococcus aureus* two-component system AgrAC displays four distinct genomic arrangements that delineate genomic virulence factor signatures. Front. Microbiol. 9, 1082.

De Alteriis, E., Lombardi, L., Falanga, A., Napolano, M., Galdiero, S., Siciliano, A., Galdiero, E., 2018. Polymicrobial antibiofilm activity of the membranotropic peptide gH625 and its analogue. Microb. Pathog. 125, 189–195.

Falanga, A., Del Genio, V., Galdiero, S., 2021. Peptides and dendrimers: How to combat viral and bacterial infections. Pharmaceutics 13 (1), 101.

Fihn, C.A., Carlson, E.E., 2021. Targeting a highly conserved domain in bacterial histidine kinases to generate inhibitors with broad spectrum activity. Curr. Opin. Microbiol. 61, 107–114.

Galanakou, C., Dhumal, D., Peng, L., 2023. Amphiphilic dendrimers against antibiotic resistance: light at the end of the tunnel?. Biomater. Sci.

Grundstad, M.L., Parlet, C.P., Kwiecinski, J.M., Kavanaugh, J.S., Crosby, H.A., Cho, Y.S., Heilmann, K., Diekema, D.J., Horswill, A.R., 2019. Quorum sensing, virulence, and antibiotic resistance of USA100 methicillin-resistant Staphylococcus aureus isolates. msphere 4 (4), 10–1128.

Janaszewska, A., Lazniewska, J., Trzepiński, P., Marcinkowska, M., Klajnert-Maculewicz, B., 2019. Cytotoxicity of dendrimers. Biomolecules 9 (8), 330.

Kadri, S.S., 2020. Key takeaways from the US CDC's 2019 antibiotic resistance threats report for frontline providers. Crit. Care Med.

Prieto, J.M., Rapún-Araiz, B., Gil, C., Penadés, J.R., Lasa, I., Latasa, C., 2020. Inhibiting the two-component system GraXRS with verteporfin to combat *Staphylococcus aureus* infections. Sci. Rep. 10 (1), 17939.

Sloan, T.J., Murray, E., Yokoyama, M., Massey, R.C., Chan, W.C., Bonev, B.B., Williams, P., 2019. Timing is everything: impact of naturally occurring *Staphylococcus aureus* AgrC cytoplasmic domain adaptive mutations on autoinduction. J. Bacteriol. 201 (20), 10–1128.

Studzian, M., Działak, P., Pułaski, Ł., Hedstrand, D.M., Tomalia, D.A., Klajnert-Maculewicz, B., 2020. Synthesis, internalization and visualization of N-(4-carbomethoxy) pyrrolidone terminated PAMAM [G5: G3-TREN] tecto (dendrimers) in mammalian cells. Molecules 25 (19), 4406.

Tiwari, S., Jamal, S.B., Hassan, S.S., Carvalho, P.V., Almeida, S., Barh, D., Azevedo, V., 2017. Two-component signal transduction systems of pathogenic bacteria as targets for antimicrobial therapy: an overview. Front. Microbiol. 8, 1878.

Xie, Q., Wiedmann, M.M., Zhao, A., Pagan, I.R., Novick, R.P., Suga, H., Muir, T.W., 2020. Discovery of quorum quenchers targeting the membrane-embedded sensor domain of the *Staphylococcus aureus* receptor histidine kinase. AgrC. Chem. Commun. 56 (76), 11223–11226.

Zhai, D., Ye, Z., Jiang, Y., Xu, C., Ruan, B., Yang, Y., Lu, Z., 2017. MOTS-c peptide increases survival and decreases bacterial load in mice infected with MRSA. Mol. Immunol. 92, 151–160.

Zhou, Y., Huang, L., Ji, S., Hou, S., Luo, L., Li, C., Jiang, L., 2019. Structural Basis for the Inhibition of the Autophosphorylation Activity of HK853 by Luteolin. Molecules 24 (5), 933.